Chapter 5
Reliability Sensitivity Analysis of Dynamical Systems

Abstract The reliability sensitivity analysis of systems subjected to stochastic loading is considered in this chapter. In particular, the change that the probability of failure undergoes due to changes in the distribution parameters of the uncertain model parameters is utilized as a sensitivity measure. A simulation-based approach that corresponds to a simple post-processing step of an advanced sampling-based reliability analysis is used to perform the sensitivity analysis. In particular, subset simulation, introduced in the previous chapter, is applied in the present formulation. The analysis does not require any additional system response evaluations. The feasibility and effectiveness of the approach is demonstrated on a finite element model of a bridge under stochastic ground excitation. The sensitivity analysis is carried out in a reduced space of generalized coordinates. The computational effort involved in the reliability sensitivity analysis of the reduced-order model is significantly decreased with respect to the corresponding analysis of the full finite element model. The reduction is accomplished without compromising the accuracy of the reliability sensitivity estimates.

5.1 Motivation

The level of safety of a structure can be measured in terms of its reliability. Even though this information is essential, it is also important to analyze the sensitivity of the reliability estimates with respect to variations in model parameters [3, 8, 13, 18, 30]. In particular, the determination of the variation in the reliability (or equivalently in the failure probability) due to changes in model parameters can provide useful information. For example, it can be used to identify the most influential model parameters and provide an important insight on system failure for risk-based decision making, such as reliability-based characterization of system responses, robust control, reliability-based design optimization, etc. [2, 6, 15, 24, 26, 34].

The subject of reliability sensitivity has been addressed in a large number of contributions. In fact, many works based on standard approximate methods such as first- and second-order reliability methods and simulation-based methods have been studied in the literature. These methods are quite general, and they have proved to

H. Jensen and C. Papadimitriou, *Sub-structure Coupling for Dynamic Analysis*,
Lecture Notes in Applied and Computational Mechanics 89,
https://doi.org/10.1007/978-3-030-12819-7_5

be very effective in a large number of problems, but their range of application is somewhat limited in the context of complex dynamical systems. A representative list of these works is included in the Refs. [1, 3–5, 13, 16, 18, 20, 22, 27, 29].

5.2 Reliability Sensitivity Analysis Formulation

As indicated in Sect. 4.1, the vector of uncertain parameters $\boldsymbol{\theta}$ is characterized in a probabilistic manner by means of a joint probability density function $q(\boldsymbol{\theta})$. For reliability sensitivity purposes, this function depends on a certain number of parameters $\boldsymbol{\tau}$, that is, $q(\boldsymbol{\theta}|\boldsymbol{\tau})$. In practice, the distribution parameters $\boldsymbol{\tau}$ can be considered, for example, as the mean value or standard deviation of $\boldsymbol{\theta}$. In this context, the mean value represents the nominal value, whereas the standard deviation models the uncertainty associated with manufacturing and construction processes. Then, it is clear that the probability of failure depends on several factors, among them, the distribution parameters $\boldsymbol{\tau}$ of the probability density function of the uncertain model parameters. Thus, the probability of failure explicitly depends on the distribution parameter vector, i.e. $P_F(\boldsymbol{\tau})$. In this manner, changes in the distribution parameters will certainly alter the response of the structure and, consequently, its probability of failure. The rate of change that the probability of failure undergoes due to these changes is denoted as reliability sensitivity analysis in the context of this chapter.

A simulation-based approach that is a simple post-processing of subset simulation is considered for performing the corresponding reliability sensitivity analysis [11]. This approach has been validated and illustrated in a series of reliability problems, including complex structural systems such as nonlinear dynamical systems under stochastic excitation and problems involving relatively large finite element models [7, 11, 20, 31]. As in the previous chapter, first excursion probabilities are used to characterize the level of safety of a structure.

5.3 Sensitivity Measure

A classical measure for sensitivity is calculating the gradient of the quantity of interest. In this context, reliability sensitivity is defined as the partial derivative of the failure probability with respect to the distribution parameters of the basic uncertain model parameters. From the definition of the probability of failure in Eq. (4.5), the sensitivity of the failure probability with respect to a distribution parameter τ_j can be written in the form

$$\left.\frac{\partial P_F(\boldsymbol{\tau})}{\partial \tau_j}\right|_{\boldsymbol{\tau}^0} = \int_{\mathbf{z}\in\Omega_z,\boldsymbol{\theta}\in\Omega_\theta} I_F(\mathbf{z},\boldsymbol{\theta})\; p(\mathbf{z})\; \frac{\partial q(\boldsymbol{\theta}|\boldsymbol{\tau})}{\partial \tau_j}\; d\mathbf{z}\; d\boldsymbol{\theta} \tag{5.1}$$

where $\boldsymbol{\tau}^0$ is the value of the distribution parameter vector where the partial derivative is evaluated, and all other terms have been previously defined. In Eq. (5.1), it has been

assumed that $q(\boldsymbol{\theta}|\boldsymbol{\tau})$ is differentiable with respect to τ_j and that the integration range does not depend on τ_j. Recall that the previous probability integral represents a high-dimensional problem in the context of dynamical systems under stochastic loading.

The sensitivity can also be defined in terms of the so-called elasticity, which is another measure usually used in the context of sensitivity analysis [7, 19]. Within this context, the elasticity e_{τ_j} of the failure probability with respect to a parameter τ_j, evaluated at $\boldsymbol{\tau}^0$, is defined as

$$e_{\tau_j} = \frac{\partial P_F}{\partial \tau_j}\bigg|_{\boldsymbol{\tau}^0} \frac{\tau_j^0}{P_F} \tag{5.2}$$

where τ_j^0 is assumed to be non-zero. This dimensionless quantity represents a more objective sensitivity measure when the uncertain model parameters are diverse in dimension. Thus, this sensitivity measure can be used to rank the importance of the model parameters on the system reliability. This measure is also less sensitive to potential bias in the failure probability estimates [7, 19].

5.4 Failure Probability Function Representation

To compute the sensitivity measure, the probability of failure $P_F(\boldsymbol{\tau})$, referred to as failure probability function, is first expressed as a function of the distribution parameter vector $\boldsymbol{\tau}$. The idea is to estimate the failure probability function by using samples and associated intermediate failure events generated by subset simulation under $q(\boldsymbol{\theta}|\boldsymbol{\tau}^0)$, that is, the probability density function of $\boldsymbol{\theta}$ with distribution parameter vector $\boldsymbol{\tau}^0$. Specifically, following the basic ideas of subset simulation (see Sect. 4.3), the probability of the first failure event F_1 can be computed as

$$\begin{aligned} P_{F_1}(\boldsymbol{\tau}) &= \int_{\mathbf{z}\in\Omega_z,\boldsymbol{\theta}\in\Omega_\theta} I_{F_1}(\mathbf{z},\boldsymbol{\theta})\; p(\mathbf{z})\; q(\boldsymbol{\theta}|\boldsymbol{\tau})\; d\mathbf{z}\; d\boldsymbol{\theta} \\ &= \int_{\mathbf{z}\in\Omega_z,\boldsymbol{\theta}\in\Omega_\theta} I_{F_1}(\mathbf{z},\boldsymbol{\theta})\; \frac{q(\boldsymbol{\theta}|\boldsymbol{\tau})}{q(\boldsymbol{\theta}|\boldsymbol{\tau}^0)}\; p(\mathbf{z}) q(\boldsymbol{\theta}|\boldsymbol{\tau}^0)\; d\mathbf{z}\; d\boldsymbol{\theta} \end{aligned} \tag{5.3}$$

where $q(\boldsymbol{\theta}|\boldsymbol{\tau}^0)$ and $q(\boldsymbol{\theta}|\boldsymbol{\tau})$ are the probability density functions of $\boldsymbol{\theta}$ with distribution parameter vector $\boldsymbol{\tau}^0$ and $\boldsymbol{\tau}$, respectively. Similarly, the probability of the conditional failure event $F_k/F_{k-1}, k = 2,\ldots,m$, can be written as

$$\begin{aligned} P_{F_k/F_{k-1}}(\boldsymbol{\tau}) &= \int_{\mathbf{z}\in\Omega_z,\boldsymbol{\theta}\in\Omega_\theta} I_{F_k}(\mathbf{z},\boldsymbol{\theta})\; p(\mathbf{z}|F_{k-1})\; q(\boldsymbol{\theta}|F_{k-1},\boldsymbol{\tau})\; d\mathbf{z}\; d\boldsymbol{\theta} \\ &= \int_{\mathbf{z}\in\Omega_z,\boldsymbol{\theta}\in\Omega_\theta} I_{F_k}(\mathbf{z},\boldsymbol{\theta})\; \frac{q(\boldsymbol{\theta}|F_{k-1},\boldsymbol{\tau})}{q(\boldsymbol{\theta}|F_{k-1},\boldsymbol{\tau}^0)}\; p(\mathbf{z}|F_{k-1}) q(\boldsymbol{\theta}|F_{k-1},\boldsymbol{\tau}^0)\; d\mathbf{z}\; d\boldsymbol{\theta} \end{aligned} \tag{5.4}$$

where $p(\mathbf{z}|F_{k-1})$ is the distribution of $\mathbf{z}$ conditional to the failure event F_{k-1}, and $q(\boldsymbol{\theta}|F_{k-1}, \boldsymbol{\tau})$ and $q(\boldsymbol{\theta}|F_{k-1}, \boldsymbol{\tau}^0)$ are the conditional distributions of $\boldsymbol{\theta}$ given that they lie in F_{k-1} under distribution parameter vectors $\boldsymbol{\tau}$ and $\boldsymbol{\tau}^0$, respectively. By definition, these conditional distributions are equal to

$$q(\boldsymbol{\theta}|F_{k-1}, \boldsymbol{\tau}) = \frac{I_{F_{k-1}}(\boldsymbol{\theta})\, q(\boldsymbol{\theta}|\boldsymbol{\tau})}{P_{F_{k-1}}(\boldsymbol{\tau})} \quad , \quad q(\boldsymbol{\theta}|F_{k-1}, \boldsymbol{\tau}^0) = \frac{I_{F_{k-1}}(\boldsymbol{\theta})\, q(\boldsymbol{\theta}|\boldsymbol{\tau}^0)}{P_{F_{k-1}}(\boldsymbol{\tau}^0)} \tag{5.5}$$

where $P_{F_{k-1}}(\boldsymbol{\tau})$ and $P_{F_{k-1}}(\boldsymbol{\tau}^0)$ are the probabilities of the failure event F_{k-1} under distribution parameter vectors $\boldsymbol{\tau}$ and $\boldsymbol{\tau}^0$ of the probability density function $q(\cdot)$, respectively. Then, the probability of the conditional failure event F_k/F_{k-1} can be given in the form

$$P_{F_k/F_{k-1}}(\boldsymbol{\tau}) = \frac{P_{F_{k-1}}(\boldsymbol{\tau}^0)}{P_{F_{k-1}}(\boldsymbol{\tau})} \int_{\mathbf{z}\in\Omega_z, \boldsymbol{\theta}\in\Omega_\theta} I_{F_k}(\mathbf{z}, \boldsymbol{\theta})\, \frac{q(\boldsymbol{\theta}|\boldsymbol{\tau})}{q(\boldsymbol{\theta}|\boldsymbol{\tau}^0)}\, p(\mathbf{z}|F_{k-1}) q(\boldsymbol{\theta}|F_{k-1}, \boldsymbol{\tau}^0)\, d\mathbf{z}\, d\boldsymbol{\theta} \tag{5.6}$$

Moreover, by definition, the probability of failure can be expressed as

$$P_F(\boldsymbol{\tau}) = P_{F_m}(\boldsymbol{\tau}) = P_{F_m/F_{m-1}}(\boldsymbol{\tau})\; P_{F_{m-1}}(\boldsymbol{\tau}) \tag{5.7}$$

Thus, from Eqs. (5.6) and (5.7) with $k = m$, it follows that

$$P_F(\boldsymbol{\tau}) = P_{F_{m-1}}(\boldsymbol{\tau}^0) \int_{\mathbf{z}\in\Omega_z, \boldsymbol{\theta}\in\Omega_\theta} I_{F_m}(\mathbf{z}, \boldsymbol{\theta})\, \frac{q(\boldsymbol{\theta}|\boldsymbol{\tau})}{q(\boldsymbol{\theta}|\boldsymbol{\tau}^0)}\, p(\mathbf{z}|F_{m-1}) q(\boldsymbol{\theta}|F_{m-1}, \boldsymbol{\tau}^0)\, d\mathbf{z}\, d\boldsymbol{\theta} \tag{5.8}$$

where from construction $P_{F_{m-1}}(\boldsymbol{\tau}^0) = p_0^{m-1}$. Then,

$$P_F(\boldsymbol{\tau}) = p_0^{m-1} \int_{\mathbf{z}\in\Omega_z, \boldsymbol{\theta}\in\Omega_\theta} I_{F_m}(\mathbf{z}, \boldsymbol{\theta})\, \frac{q(\boldsymbol{\theta}|\boldsymbol{\tau})}{q(\boldsymbol{\theta}|\boldsymbol{\tau}^0)}\, p(\mathbf{z}|F_{m-1}) q(\boldsymbol{\theta}|F_{m-1}, \boldsymbol{\tau}^0)\, d\mathbf{z}\, d\boldsymbol{\theta} \tag{5.9}$$

The last equation represents an analytical characterization, in the framework of subset simulation, of the failure probability function in terms of the distribution parameter vector $\boldsymbol{\tau}$.

5.5 Sensitivity Estimation

Using the previous characterization of the failure probability function, the partial derivative of $P_F(\boldsymbol{\tau})$ with respect to τ_j, evaluated at $\boldsymbol{\tau}^0$, can be written as

$$\left.\frac{\partial P_F}{\partial \tau_j}\right|_{\boldsymbol{\tau}^0} = p_0^{m-1} \int_{\mathbf{z}\in\Omega_z, \boldsymbol{\theta}\in\Omega_\theta} I_{F_m}(\mathbf{z}, \boldsymbol{\theta})\, \frac{\frac{\partial q}{\partial \tau_j}(\boldsymbol{\theta}|\boldsymbol{\tau}^0)}{q(\boldsymbol{\theta}|\boldsymbol{\tau}^0)}\, p(\mathbf{z}|F_{m-1}) q(\boldsymbol{\theta}|F_{m-1}, \boldsymbol{\tau}^0)\, d\mathbf{z}\, d\boldsymbol{\theta} \tag{5.10}$$

or in terms of the expectation operator

$$\left.\frac{\partial P_F}{\partial \tau_j}\right|_{\boldsymbol{\tau}^0} = p_0^{m-1} E_{p(\mathbf{z}|F_{m-1}),q(\boldsymbol{\theta}|F_{m-1},\boldsymbol{\tau}^0)}\left[I_{F_m}(\mathbf{z},\boldsymbol{\theta})\ \frac{\frac{\partial q}{\partial \tau_j}(\boldsymbol{\theta}|\boldsymbol{\tau}^0)}{q(\boldsymbol{\theta}|\boldsymbol{\tau}^0)} \right] \tag{5.11}$$

where $E_{p(\mathbf{z}|F_{m-1}),q(\boldsymbol{\theta}|F_{m-1},\boldsymbol{\tau}^0)}[\,\cdot\,]$ is the expectation operator with respect to the distributions $p(\mathbf{z}|F_{m-1})$ and $q(\boldsymbol{\theta}|F_{m-1},\boldsymbol{\tau}^0)$. From the last expression, the sensitivity can be estimated as

$$\left.\frac{\partial P_F}{\partial \tau_j}\right|_{\boldsymbol{\tau}^0} \approx p_0^{m-1}\ \frac{1}{N_m}\sum_{i=1}^{N_m} I_{F_m}(\mathbf{z}_{m-1,i},\boldsymbol{\theta}_{m-1,i}^0)\frac{\frac{\partial q}{\partial \tau_j}(\boldsymbol{\theta}_{m-1,i}^0|\boldsymbol{\tau}^0)}{q(\boldsymbol{\theta}_{m-1,i}^0|\boldsymbol{\tau}^0)} \tag{5.12}$$

where $\{(\mathbf{z}_{m-1,i},\boldsymbol{\theta}_{m-1,i}^0), i=1,\ldots,N_m\}$ is the set of samples generated at the last stage of subset simulation under distribution parameter vector $\boldsymbol{\tau}^0$ of the probability density function $q(\cdot)$, and all other terms have been previously defined.

It is observed that a single subset simulation analysis is required for estimating the sensitivity of the probability of failure with respect to the distribution parameters. Therefore, the reliability sensitivity analysis is a simple post-processing of a sampling-based reliability analysis. In other words, the approach does not require any additional sampling of the indicator function (dynamic analysis). In summary, it is seen that the estimation of the failure probability and its gradient can be done with the same samples generated at the last stage of subset simulation. The previous approach can be extended to higher-order derivatives provided that the distribution $q(\boldsymbol{\theta}|\boldsymbol{\tau})$ is sufficiently differentiable. It is noted that the characterization of the partial derivative of the failure probability function with respect to the jth component of $\boldsymbol{\tau}$ (see Eq. (5.10)) can be also expressed in terms of the so-called score function, which is the partial derivative of the logarithm of the distribution $q(\boldsymbol{\theta}|\boldsymbol{\tau}^0)$ [25].

5.6 Sensitivity Versus Threshold

From the formulation of subset simulation (see Sect. 4.3.2), it is clear that the demand function values $\delta_1,\ldots,\delta_m$ at specified probability levels are the ones that are estimated, rather than the conditional failure probabilities. Consequently, subset simulation serves as a method to generate random samples whose response values correspond to specified probability levels, rather than a technique to estimate failure probabilities for specified failure events. As a result, it produces information about the probability of failure versus the threshold and not only for a single value. Since the proposed reliability sensitivity analysis is based on subset simulation, a similar information can be obtained for the sensitivity measures.

For a demand function value $\bar{\delta}$ such that $\delta_{k-1} < \bar{\delta} \le \delta_k, k=1,\ldots,m$, with $\delta_0 = 0$, the partial derivative of $P_F(\boldsymbol{\tau})$ with respect to τ_j, evaluated at $\boldsymbol{\tau}^0$, can be

estimated as [11, 12]

$$\left.\frac{\partial P_F}{\partial \tau_j}\right|_{\boldsymbol{\tau}^0} \approx p_0^{k-1}\ \frac{1}{N_k}\sum_{i=1}^{N_k} I_{\bar{F}}(\mathbf{z}_{k-1,i}, \boldsymbol{\theta}_{k-1,i}^0)\frac{\frac{\partial q}{\partial \tau_j}(\boldsymbol{\theta}_{k-1,i}^0|\boldsymbol{\tau}^0)}{q(\boldsymbol{\theta}_{k-1,i}^0|\boldsymbol{\tau}^0)} \tag{5.13}$$

where $\bar{F}$ is the failure event defined as

$$\bar{F} = \left\{d(\mathbf{z}, \boldsymbol{\theta}) > \bar{\delta}\right\} \tag{5.14}$$

and $\{(\mathbf{z}_{k-1,i}, \boldsymbol{\theta}_{k-1,i}^0), i = 1, \ldots, N_k\}$ is the set of samples generated at level $k-1$ of subset simulation under distribution parameter vector $\boldsymbol{\tau}^0$ of the probability density function $q(\cdot)$. In this manner, a single simulation run yields reliability sensitivity estimates for all thresholds up to the largest one considered in the analysis. In other words, the whole trend of the sensitivity measure versus the thresholds can be obtained in a direct manner. This feature of the approach is quite desirable because it provides much more information than a point estimate.

5.7 Particular Cases

The previous general formulation can be specialized for different probability distributions of the uncertain model parameters and different distribution parameters as long as Eq. (5.1) holds. Of practical importance is the case when the distribution parameters are represented by the mean values and standard deviations of the system parameters. These distribution parameters can be considered as a control or design variables in a number of important applications such as reliability sensitivity analysis, reliability-based characterization of structural responses, reliability-based design optimization, robust solutions and predictions, robust design optimization, etc. For illustration purposes, some sensitivity measures corresponding to the case of normal and log-normal random variables are given in the following equations.

The partial derivatives of the failure probability with respect to the mean value μ_{θ_j} and standard deviation σ_{θ_j} of the model parameter θ_j, evaluated at $\mu_{\boldsymbol{\theta}}^0$ and $\sigma_{\boldsymbol{\theta}}^0$ for the case of a normal random variable are estimated as [11, 12]

$$\left.\frac{\partial P_F}{\partial \mu_{\theta_j}}\right|_{\mu_{\boldsymbol{\theta}}^0} \approx p_0^{m-1}\ \frac{1}{N_m}\sum_{i=1}^{N_m} I_F(\mathbf{z}_{m-1,i}, \boldsymbol{\theta}_{m-1,i}^0) \times \left\{\frac{(\theta_{m-1,ij}^0 - \mu_{\theta_j}^0)}{{\sigma_{\theta_j}^0}^2}\right\} \tag{5.15}$$

and

$$\left.\frac{\partial P_F}{\partial \sigma_{\theta_j}}\right|_{\sigma_{\boldsymbol{\theta}}^0} \approx p_0^{m-1} \frac{1}{N_m} \sum_{i=1}^{N_m} I_F\left(\mathbf{z}_{m-1,i}, \boldsymbol{\theta}_{m-1,i}^0\right) \times \left\{ \frac{(\theta_{m-1,ij}^0 - \mu_{\theta_j}^0)^2}{{\sigma_{\theta_j}^0}^2} - 1 \right\} \frac{1}{\sigma_{\theta_j}^0} \tag{5.16}$$

where $\{(\mathbf{z}_{m-1,i}, \boldsymbol{\theta}_{m-1,i}^0), i = 1, \ldots, N_m\}$ is the set of samples generated at the last stage of subset simulation under distributions $p(\mathbf{z}|F_{m-1})$ and $q(\boldsymbol{\theta}|F_{m-1}, \boldsymbol{\tau}^0)$, respectively, and $\boldsymbol{\theta}_{m-1,ij}^0$ is the jth component of the sample vector $\boldsymbol{\theta}_{m-1,i}^0$.

For the case of a log-normal random variable, the estimators are written as [11, 12]

$$\left.\frac{\partial P_F}{\partial \mu_{\theta_j}}\right|_{\mu_{\boldsymbol{\theta}}^0} \approx p_0^{m-1} \frac{1}{N_m} \sum_{i=1}^{N_m} I_F(\mathbf{z}_{m-1,i}, \boldsymbol{\theta}_{m-1,i}^0) \times \left\{ \left[\frac{(\ln(\theta_{m-1,ij}^0) - \mu_j)}{{\sigma_j}^2} \right] \alpha_j + \left[\frac{(\ln(\theta_{m-1,ij}^0) - \mu_j)^2}{{\sigma_j}^2} - 1 \right] \frac{1}{\sigma_j^2} \beta_j \right\} \tag{5.17}$$

and

$$\left.\frac{\partial P_F}{\partial \sigma_{\theta_j}}\right|_{\sigma_{\boldsymbol{\theta}}^0} \approx p_0^{m-1} \frac{1}{N_m} \sum_{i=1}^{N_m} I_F\left(\mathbf{z}_{m-1,i}, \boldsymbol{\theta}_{m-1,i}^0\right) \times \left\{ \left[\frac{(\ln(\theta_{m-1,ij}^0) - \mu_j)}{\sigma_j^2} \right] \lambda_j - \left[\frac{(\ln(\theta_{m-1,ij}^0) - \mu_j)^2}{\sigma_j^2} - 1 \right] \frac{1}{\sigma_j^2} \lambda_j \right\} \tag{5.18}$$

where

$$\alpha_j = \left[2 - \exp\left(-{\sigma_j}^2\right)\right] \exp\left(-\left(\mu_j + {\sigma_j}^2/2\right)\right) \tag{5.19}$$

$$\beta_j = \left[\exp\left(-{\sigma_j}^2\right) - 1\right] \exp\left(-\left(\mu_j + {\sigma_j}^2/2\right)\right) \tag{5.20}$$

$$\lambda_j = -[\exp(\sigma_j^2) - 1]^{1/2} \exp(-(\mu_j + 3\sigma_j^2/2)) \tag{5.21}$$

with

$$\mu_j = \ln\left(\left(\mu_{\theta_j}^0\right)^2 / \sqrt{\left(\mu_{\theta_j}^0\right)^2 + \left(\sigma_{\theta_j}^0\right)^2} \right) \tag{5.22}$$

$$\sigma_j = \sqrt{\ln\left(1 + \left(\sigma_{\theta_j}^0 / \mu_{\theta_j}^0\right)^2\right)} \tag{5.23}$$

and all other terms have been previously defined. Similar expressions can be derived for higher order derivatives and for other types of probability distributions of the uncertain model parameters provided that the distribution $q(\boldsymbol{\theta}|\boldsymbol{\tau})$ is sufficiently differentiable.

5.8 Application Problem

The objective of the application problem is to determine the feasibility and effectiveness of the proposed reliability sensitivity analysis approach in an involved model. Even though the proposed sensitivity analysis is a simple post-processing of the subset simulation, it can be computationally very demanding due to the large number of dynamic analyses required during the reliability sensitivity estimation (evaluation of the indicator function). Therefore, the total computational demand may become excessive when the computational time for performing a dynamic finite element analysis is significant. To deal with this difficulty, the reliability sensitivity analysis is carried out in a reduced-order model.

5.8.1 Model Description

A three-dimensional bridge finite element model of 10,068 degrees of freedom is considered in the application problem. The bridge model, shown in Fig. 5.1, is curved in plan and has a total length of 119 m. It has five spans of lengths equal to 24 m, 20 m, 23 m, 25 m, and 27 m, respectively, and four piers of 8 m height that monolithically support the girder. Each pier is founded on an array of four piles

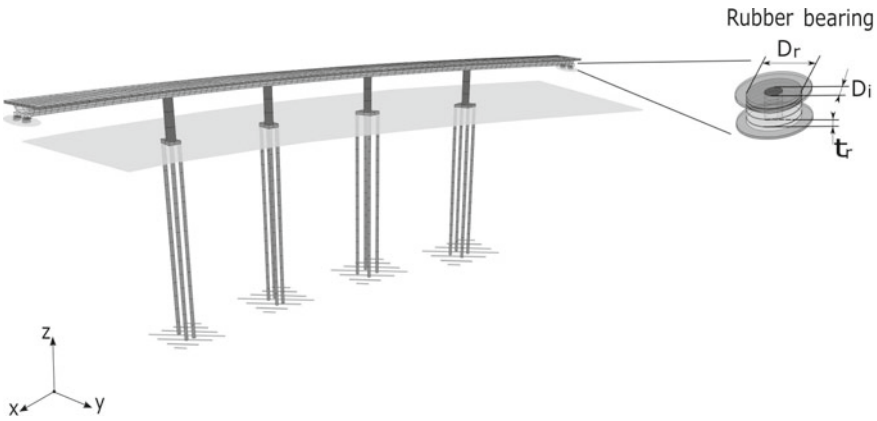

Fig. 5.1 Finite element model of bridge structure

of 35 m height. The piers and piles are modeled as column elements of circular cross-section with $D_c = 1.6\,\text{m}$ and $D_p = 0.6\,\text{m}$ diameter, respectively, while the deck cross-section is a box girder. The deck girder is modeled by beam and shell elements and rests on each abutment through two rubber bearings, which are used as an isolation system.

The rubber bearings consist of layers of rubber and steel, with the rubber being vulcanized to the steel plates. A schematic representation of a rubber bearing is also shown in the figure, where D_r represents the external diameter, D_i is the internal diameter, and $H_r = t_r n_r$ is the total height of rubber in the bearing where t_r is the layer thickness and n_r is the number of rubber layers. The nominal values of the rubber bearings parameters are set equal to $D_r = 0.80\,\text{m}$, $D_i = 0.10\,\text{m}$, and $H_r = 0.17\,\text{m}$. The interaction between the piles and the soil is modeled by a series of translational springs in the x and y direction along the height of the piles, with stiffnesses varying linearly from $K_s = 11{,}200\,\text{T/m}$ at the base to 0 at the surface. The net effect of these elements is to increase the translational stiffness of the column elements that model the piles. Material properties of the structural model have been assumed as follows: Young's modulus $E = 2.0 \times 10^{10}\,\text{N/m}^2$; Poisson's ratio $\nu = 0.2$, and mass density $\rho = 2{,}500\,\text{kg/m}^3$. In addition, 3% of critical damping is added to the model. It is assumed that the structural components, such as the piers, piles, and the deck girder, remain linear during the analysis, while the nonlinearities are localized in the rubber bearings response. In addition, the axial deformation of the piers and piles is neglected with respect to their bending deformation.

The bridge structure is subjected to a ground acceleration applied in a direction defined at 25° with respect to the x-axis. It is modeled as the non-stationary stochastic process described in Sect. 4.5. The values of the various parameters involved in the model are taken as the ones considered in the previous chapter. The duration of the excitation is taken equal to $T = 30$ s with a sampling interval equal to $\Delta T = 0.01$ s. Thus, the vector of uncertain parameters $\mathbf{z}$ involves more than 3,000 uncertain parameters, as $\mathbf{z}^T =< z_1, z_2, \ldots, z_{3001} >$. Consequently, the corresponding reliability problem and, therefore, the reliability sensitivity analysis problem is high-dimensional.

5.8.2 Rubber Bearings

5.8.2.1 Description

Rubber bearings have been used over many years in a number of seismically isolated structures worldwide [14, 21, 28]. They require minimal initial cost and maintenance compared to other passive, semi-active, and active energy absorption devices. Rubber bearing systems, in principle, are able to provide horizontal flexibility together with the restoring force and supply the required hysteretic damping. An analytical model that simulates measured restoring forces under bidirectional loadings is considered. The model is based on a series of experimental tests conducted for real-size rubber

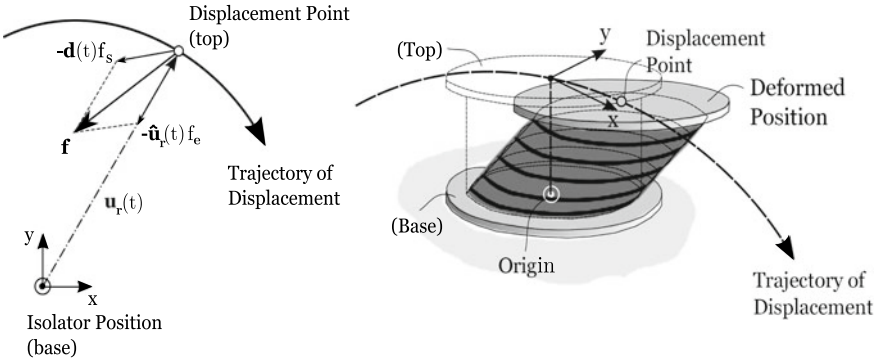

Fig. 5.2 Decomposition of the restoring force

bearings [23, 32]. The loading tests of seven full-scale isolators were carried out using the Caltrans Seismic Response Modification Device Test Facility at the University of California, San Diego. The specimens used in the tests were made with high damping rubber compounds. In particular, horizontal bidirectional loading tests for isolators with a diameter of 0.7 m and 1.3 m were conducted. On the basis of the test results, the model assumes that the restoring force on the rubber bearing is composed of a force directed to the origin of the isolator and another force approximately opposite to the direction of the movement of the isolator. This decomposition of the restoring force is schematically shown in Fig. 5.2.

According to the model, a vector approximately in the direction of the motion $\mathbf{d}(t)$, can be defined in terms of the isolator displacement vector $\mathbf{u}_r(t)$ in the x and y direction by means of the nonlinear differential equation [9, 10, 33]

$$\dot{\mathbf{d}}(t) = \frac{1}{\alpha} \parallel \dot{\mathbf{u}}_r(t) \parallel \left[\hat{\dot{\mathbf{u}}}_r(t) - \parallel \mathbf{d}(t) \parallel^{\beta} \hat{\mathbf{d}}(t) \right] , \ \mathbf{u}_r(0) = \mathbf{0} , \ \mathbf{d}(0) = \mathbf{0} \tag{5.24}$$

where $\dot{\mathbf{u}}_r(t)$ is the velocity vector, $\hat{\dot{\mathbf{u}}}_r(t)$ and $\hat{\mathbf{d}}(t)$ are the unit directional vectors of $\dot{\mathbf{u}}_r(t)$ and $\mathbf{d}(t)$, respectively, and $\| \cdot \|$ indicates the Euclidean norm. The parameters α and β are positive constants that relate to the yield displacement and smoothness of yielding, respectively. Once the vector $\mathbf{d}(t)$ has been derived, the restoring force $\mathbf{f}(t)$ on the isolator (in the x and y direction) is expressed in terms of the unit directional vector $\hat{\mathbf{u}}_r(t)$ and the vector $\mathbf{d}(t)$ as

$$\mathbf{f}(t) = -\hat{\mathbf{u}}_r(t) f_e(t) - \mathbf{d}(t) f_s(t) \tag{5.25}$$

where $f_e(t)$ is the nonlinear elastic component and $f_s(t)$ is the elastoplastic component. Based on the results reported in [33], it was concluded that the model is able to accurately simulate the test results for both bidirectional and unidirectional loading.

5.8.2.2 Model Parameter Identification and Validation

The mathematical model for the description of the isolator behavior can be used to calibrate the model parameters by using a specific set of loading tests carried out for real-size bearings. First, the parameters α and β, which define the transition curve from the elastic to inelastic regime, are calibrated. They are estimated as $0.2H_r$ and 0.7, respectively, where H_r is the total height of rubber, as indicated before [33]. Next, the stress-strain relationships for $\tau_e(t) = f_e(t)/A$, and $\tau_s(t) = f_s(t)/A$ are calibrated by means of quadratic and cubic curves as [17]

$$\tau_e(t) = \begin{cases} 0.35\gamma(t) & \text{if } 0 \le \gamma(t) \le 1.8 \\ 0.35\gamma(t) + 0.2(\gamma(t) - 1.8)^2 & \text{if } \gamma(t) \ge 1.8 \end{cases} \tag{5.26}$$

and

$$\tau_s(t) = 0.125 + 0.015\gamma(t) + 0.012\gamma(t)^3 \tag{5.27}$$

where A is the cross-sectional area of the rubber, and $\gamma(t) = \| \mathbf{u}_r(t) \| / H_r$ is the average shear-strain. The test results show that the scatter of the experimental data around these calibrated curves is relatively small for average shear strains of less than 200%. Test-restoring forces and those calculated by the model under unidirectional loading are compared in Fig 5.3 for two specimens. They correspond to a medium- and large-sized rubber bearing, respectively. The test results were conducted for a maximum average shear strain of 150%. It is seen that the analytical model simulates the test results very well. The extra loop shown in the figures is generated by the analytical model to illustrate the predicted behavior of the rubber bearings for large average shear strains (250%). Additional validation calculations have shown that the

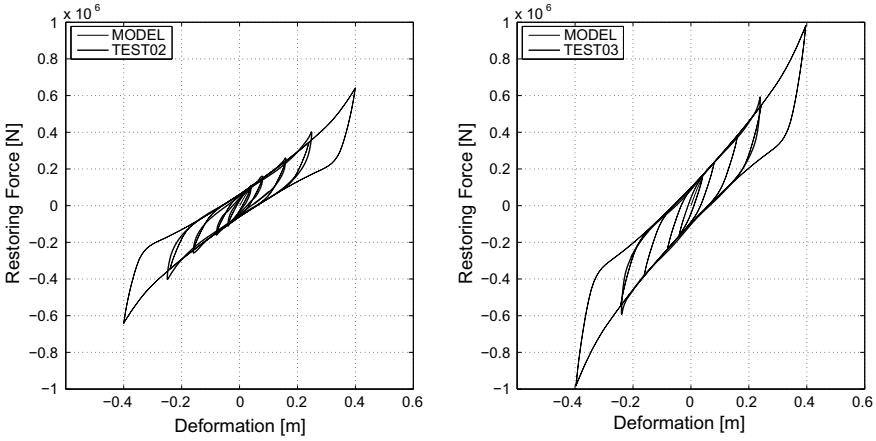

Fig. 5.3 Comparison of analytical and experimental hysteresis loops. Left figure: medium size rubber bearing. $D_r = 0.8\,\text{m}$, $H_r = 0.16\,\text{m}$, $D_i = 0.15\,\text{m}$. Right figure: large size rubber bearing. $D_r = 1.0\,\text{m}$, $H_r = 0.16\,\text{m}$, $D_i = 0.15\,\text{m}$

analytical model is also able to accurately simulate the test results for bidirectional loadings [9, 10, 33].

5.8.3 Reliability Sensitivity Analysis Formulation

The performance of the bridge structure is characterized in terms of the probability of occurrence of three failure events. The events are related to the maximum absolute acceleration at the middle of the deck girder, the maximum relative displacement between the top of the piers and their connections with the pile foundation, and the maximum relative displacement between the deck girder and the base of the rubber bearings at each abutment. Mathematically, the failure events are defined as

$$\begin{aligned} F_1(\mathbf{z}, \boldsymbol{\theta}) &= \left\{ \max_{t\in[0,T]} \left(\left| \frac{\ddot{x}_{\text{absolute}}(t, \mathbf{z}, \boldsymbol{\theta})}{2.00\,\text{m/s}^2} \right| \right) > 1 \right\}, \\ F_2(\mathbf{z}, \boldsymbol{\theta}) &= \left\{ \max_{t\in[0,T]} \left(\left| \frac{\delta x(t, \mathbf{z}, \boldsymbol{\theta})}{0.07\,\text{m}} \right| \right) > 1 \right\}, \\ F_3(\mathbf{z}, \boldsymbol{\theta}) &= \left\{ \max_{t\in[0,T]} \left(\left| \frac{\delta r(t, \mathbf{z}, \boldsymbol{\theta})}{0.10\,\text{m}} \right| \right) > 1 \right\} \end{aligned} \tag{5.28}$$

where $\ddot{x}_{\text{absolute}}(t, \mathbf{z}, \boldsymbol{\theta})$ represents the absolute acceleration at the middle of the deck girder (in the x or y direction), $\delta x(t, \mathbf{z}, \boldsymbol{\theta})$ denotes the relative displacement between the top of the piers and their connections with the pile foundation (in the x or y direction), and $\delta r(t, \mathbf{z}, \boldsymbol{\theta})$ describes the relative displacement between the deck girder and the base of the rubber bearings at each abutment (in the x or y direction). It is expected that system parameters, such as the diameter of the pier elements, the diameter of the pile elements, the external diameter of the rubber bearings, and the total height of rubber in the bearing, may have important effects on the system response. Thus, a reliability sensitivity analysis with respect to these parameters may provide important information about the overall behavior of the bridge structure. Based on the previous observations, the vector of the system parameters is defined as $\boldsymbol{\theta}^T =< D_c, D_p, D_r, H_r >$. To study the behavior of the failure probability when the system parameters vary in a certain region of the parameters space, the system parameters are modeled as independent normal random variables with distribution parameters given in Table 5.1. Of course, alternative distributions can also be used. Note that the uncertainty associated with the system parameters D_c, D_p, D_r and H_r (geometrical parameters) may correspond to the inherent variability in the construction process of these elements (piers, piles, and rubber bearings), or they may be considered as an instrumental variability in the context of this analysis.

Table 5.1 Distribution of system parameters

System parameter	Mean value	C.O.V.
D_c (diameter of pier elements)	$\mu_{D_c} = 1.6\,\text{m}$	0.10
D_p (diameter of pile elements)	$\mu_{D_p} = 0.6\,\text{m}$	0.10
D_r (external diameter of rubber bearings)	$\mu_{D_r} = 0.8\,\text{m}$	0.10
H_r (total height of rubber)	$\mu_{H_r} = 0.16\,\text{m}$	0.10

5.8.4 *Reduced-Order Model*

To carry out the reliability sensitivity analysis in a reduced-order model, the bridge model is divided into a number of substructures. In particular, the structural model is subdivided into nine linear substructures and two nonlinear substructures, as shown in Fig. 5.4.

Substructures S_1, S_2, S_3, and S_4 are composed of the different pile elements, substructures S_5, S_6, S_7 and S_8 include the different pier elements, and substructure S_9 corresponds to the deck girder. Finally, substructures S_{10} and S_{11} are the nonlinear substructures composed of the rubber bearings located at the left and right abutment, respectively. Based on the previous definition of substructures, it is clear that substructures S_1, S_2, S_3, and S_4 depend on the system parameter D_p, substructures S_5, S_6, S_7 and S_8 depend on the system parameter D_c, while substructure S_9 is independent of the system parameters. Furthermore, the nonlinear substructures depend on the system parameters D_r and H_r. In connection with Chap. 2, the corresponding parametrization functions are given by $h^j(\theta_j) = \theta_j^4$ (parameter related to the inertia

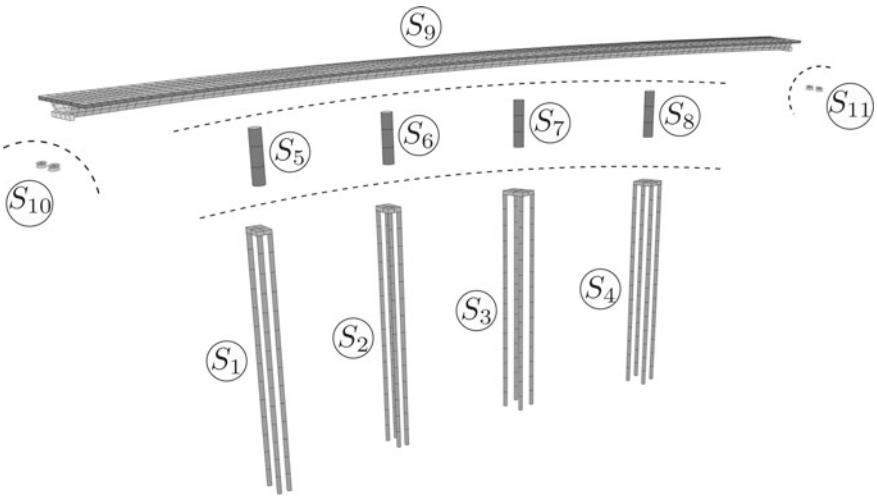

Fig. 5.4 Linear and nonlinear substructures of the finite element model

Table 5.2 Modal frequency difference between the modal frequencies of the full model and the reduced-order model based on dominant fixed-interface modes

Frequency number	Unreduced model	Reduced-order model	Error
	ω (rad/s)	ω (rad/s)	| Difference |
1	4.214	4.216	2.0×10^{-3}
2	4.282	4.284	2.0×10^{-3}
3	4.569	4.572	3.0×10^{-3}
4	12.197	12.249	5.2×10^{-2}
5	15.424	15.462	3.8×10^{-2}
6	23.419	23.421	2.0×10^{-3}

term in the stiffness matrices) and $g^j(\theta_j) = \theta_j^2$ (parameter related to the area term in the mass matrices), where the model parameter θ_j is either D_c or D_p, normalized by its mean value.

Validation calculations indicate that retaining three generalized coordinates (dominant fixed-interface normal modes) for each one of substructures S_1, S_2, S_3, and S_4, two for each one of substructures S_5, S_6, S_7 and S_8, and 10 for substructure S_9 are adequate in the context of this application. The absolute value of the difference between the modal frequencies using the full nominal reference finite element model and the modal frequencies computed using the reduced-order model based on dominant fixed-interface normal modes is shown in Table 5.2. The modal frequencies for both models are computed by considering only the linear components of the structural system. A small difference is observed with this number of generalized coordinates. The corresponding matrix of MAC-values between the first six modal vectors com-

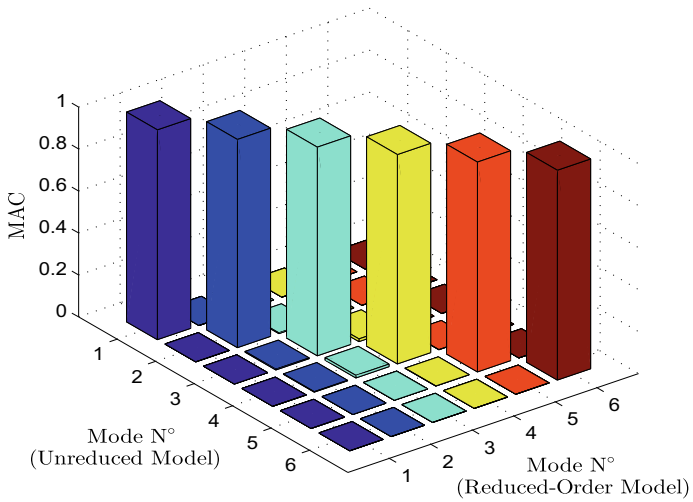

Fig. 5.5 MAC-values between the mode shapes computed from the unreduced finite element model and from the reduced-order model based on dominant fixed-interface modes

puted from the unreduced finite element model and from the reduced-order model is shown in terms of a 3-D representation in Fig. 5.5.

It is observed that the values at the diagonal terms are close to one and almost zero at the off-diagonal terms. Thus, the modal vectors of both models are consistent. The comparison with the lowest six modes is based on the fact that the contribution of the higher order modes (higher than the 6th mode) in the dynamic response of the model is negligible. In fact, the dynamic response of the magnitudes associated with the failure events, that is, $\ddot{x}_{\text{absolute}}(t, \mathbf{z}, \boldsymbol{\theta})$, $\delta x(t, \mathbf{z}, \boldsymbol{\theta})$, and $\delta r(t, \mathbf{z}, \boldsymbol{\theta})$, obtained from the reduced-order model, coincides with the response obtained from the unreduced finite element model. Note that residual normal modes and interface modes are not involved in the construction of the reduced-order model. In summary, a total of 30 generalized coordinates, corresponding to the fixed-interface normal modes of the linear substructures, out of 10,008 internal degrees of freedom of the original model, are retained for the nine linear substructures. Therefore, the number of interface degrees of freedom is equal to 60 in this case. With this reduction, the total number of generalized coordinates of the reduced-order model represents a 99% reduction with respect to the unreduced model. Thus, a drastic reduction in the number of generalized coordinates is obtained with respect to the number of the degrees of freedom of the original unreduced finite element model. Based on the previous analysis, it is concluded that the reduced-order model and the full finite element model are equivalent in the context of this application problem. Therefore, the reliability sensitivity analysis of the bridge structural model is carried out by using the reduced-order model. From the practical point of view, it is important to note that the selection of the fixed-interface modes per substructure, necessary to achieve a prescribed accuracy, can be done offline, before the reliability sensitivity analysis takes place.

In the following, the reliability sensitivity analysis corresponding to the three failure events is presented. The sensitivity measures with respect to a given parameter are estimated by considering the other parameters fixed at their mean values. This is done to isolate the effect of the parameter variation on the system reliability.

Table 5.3 Sensitivity measures in terms of partial derivatives. $(\cdot\%)$ sample coefficient of variation. Failure event F_1

Average value (c.o.v.)
$\frac{\partial P_{F_1}}{\partial \mu_{D_p}}$ 3.85×10^{-2} (27%)
$\frac{\partial P_{F_1}}{\partial \mu_{D_c}}$ 5.37×10^{-3} (47%)

Table 5.4 Sensitivity measures in terms of elasticity coefficients. $(\cdot\%)$ sample coefficient of variation. Failure event F_1

Average value (c.o.v.)
$e^{F_1}_{\mu_{D_p}}$ 7.26 (21%)
$e^{F_1}_{\mu_{D_c}}$ 3.28 (47%)

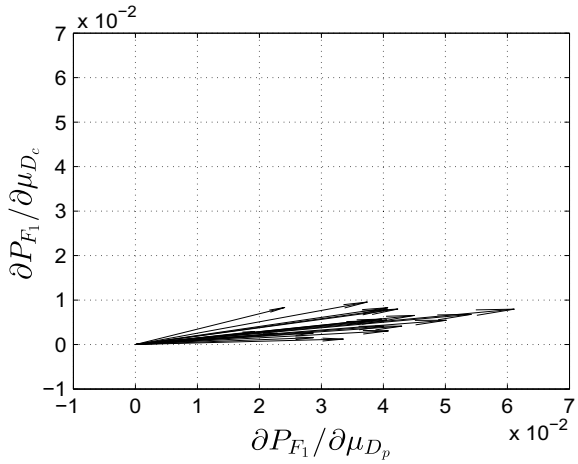

Fig. 5.6 Sensitivity of the failure probability P_{F_1} with respect to the mean value of the diameter of the pier and pile elements: 20 independent estimations

5.8.5 *Results: Failure Event* F_1

The results of the reliability sensitivity analysis corresponding to the failure event associated with the maximum absolute acceleration at the middle of the deck girder are given in Tables 5.3 and 5.4.

Table 5.3 shows the sensitivity analysis in term of the partial derivatives of the failure probability with respect to the mean value of the system parameters D_p and D_c, while Table 5.4 gives the corresponding sensitivity measures in terms of the elasticity coefficients. The proposed approach is implemented by using 1,000 samples at each conditional level of subset simulation with conditional failure probabilities equal to $p_0 = 0.1$. The estimates shown in the tables correspond to an average of 20 independent runs. The sensitivity information provided in Tables 5.3 and 5.4 is also showed in Fig. 5.6 in form of arrows indicating the magnitude and sign of the sensitivity. Twenty representative estimations are considered in the figure.

It is observed that the sensitivity measures with respect to the mean value of the parameters D_p and D_c are positive. Thus, an increase in the value of these parameters increases the probability of failure. In fact, an increase in the diameter of the pier and pile elements tends to increase the maximum absolute acceleration at the middle of the deck girder, which is reasonable from a structural point of view. It is also seen that failure appears to be most sensitive to the mean value of the diameter of the piles, as expected. The estimates generated by the proposed simulation-based approach present some level of dispersion, which can be observed from Fig. 5.6. However, on average, the estimates converge to the reference value. This result is shown in Fig. 5.7 in terms of the elasticity coefficient estimates, where the reference result is obtained directly by Monte Carlo simulation with a large number of samples (100,000 in this case). The corresponding direct simulation is carried out by using the reduced-order model. The actual variability of the sensitivity estimates is given in parentheses in Tables 5.3 and 5.4. That number corresponds to the sample coefficient of variation of the estimates over 20 independent runs.

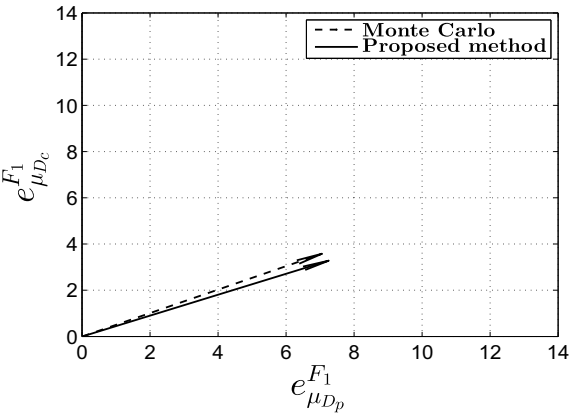

Fig. 5.7 Average of the elasticity coefficient estimates generated by the proposed approach from 20 simulation runs compared to the reference estimate (Monte Carlo). Failure event F_1. System parameters D_p and D_c

A similar reliability sensitivity analysis can be performed with respect to the standard deviation of the system parameters D_p and D_c. It turns out that the elasticity of the failure probability with respect to the standard deviation of these parameters is positive. Therefore, the probability of failure increases, i.e., the structural reliability reduces, with an increase in the standard deviation (variability) of the diameters of the pier and pile elements. The information provided by the sensitivity analysis with respect to the standard deviation of the system parameters can be used to identify the parameters whose uncertainty plays a major role in affecting the failure probability.

As stated in Sect. 5.6, the proposed method yields with a single subset simulation run reliability sensitivity estimates for all thresholds up to the largest one considered in the analysis. In this context, Figs. 5.8 and 5.9 show the probability of failure and the corresponding elasticity coefficients in terms of the threshold. The results with respect to the mean value of the diameter of the pile elements are shown in Fig. 5.8, while Fig. 5.9 shows the results related to the mean value of the diameter of the pier elements. In these figures, an average of 20 independent runs is considered, where the threshold is normalized by the acceptable acceleration response level equal to 2.0 m/s^2 (see Sect. 5.8.3). These figures illustrate the whole trend of the probability of failure and sensitivity measure in terms of the threshold, not only for the normalized target value equal to one. This feature of the proposed method is quite useful, since the whole trend of the sensitivity measures versus the threshold is obtained. It is observed from the figures that the elasticity coefficients increase as the threshold level increases and, therefore, the failure probability becomes more sensitive as the failure probability becomes smaller.

5.8.6 Results: Failure Event F_2

The results of the reliability sensitivity analysis associated with the second failure event are given in Tables 5.5 and 5.6. Table 5.5 shows the sensitivity analysis in terms

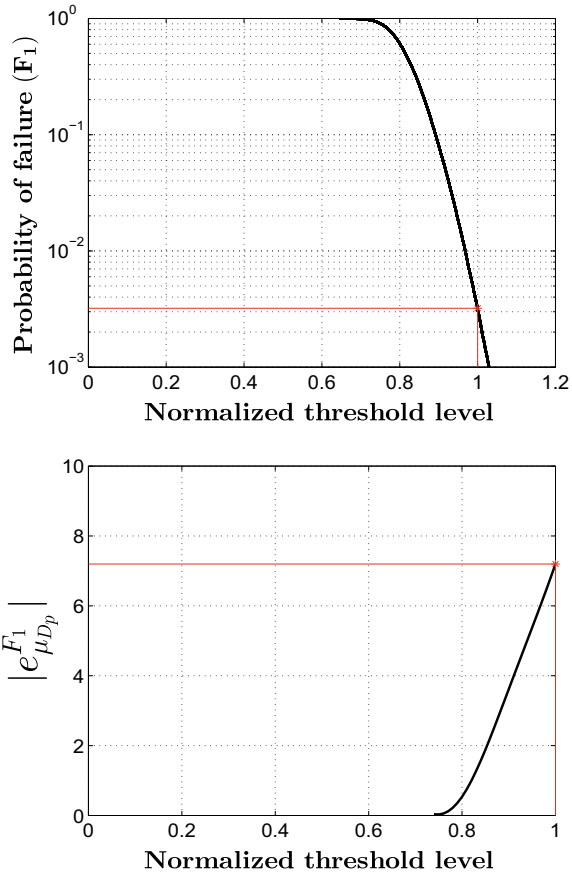

Fig. 5.8 Upper figure: Probability of failure event F_1 in terms of the normalized threshold. Lower figure: Elasticity coefficient of failure probability P_{F_1} in terms of the normalized threshold. System parameter D_p (diameter of pile elements)

of the partial derivatives of the failure probability with respect to the mean value of the system parameters D_p and D_c, while Table 5.6 gives the corresponding sensitivity measures in terms of the elasticity coefficients.

This information is also shown in Fig. 5.10 in form of arrows indicating the magnitude and sign of the sensitivity. As in the previous case, the results are based on 20 independent runs. For this failure event, the sensitivity measures with respect to the mean value of the parameters D_p and D_c are negative. Thus, an increase in the value of these parameters decreases the probability of failure. In this case, an increase in the diameter of the pier and pile elements tends to decrease the maximum relative displacement between the piers and the piles, as expected. The results indicate that both parameters, that is, the mean value of the diameter of the pile and pier elements, have an important effect on P_{F_2}.

A close examination of the results reveals that the probability of failure event F_2 is more sensitive to the diameter of the pier elements than to the diameter of the pile elements, which makes sense from a physical point of view. The numerical results also show that, on average, the estimates obtained from the proposed approach

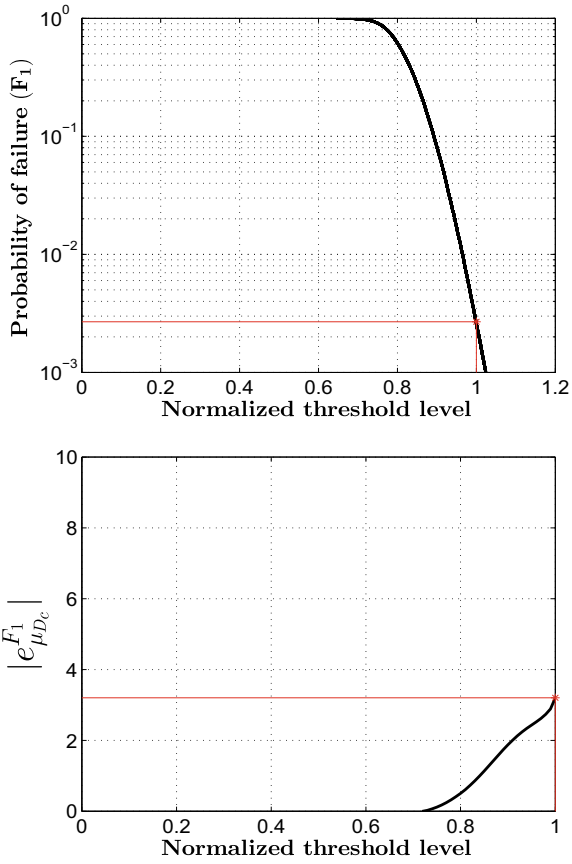

Fig. 5.9 Upper figure: Probability of failure event F_1 in terms of the normalized threshold. Lower figure: Elasticity coefficient of failure probability P_{F_1} in terms of the normalized threshold. System parameter D_c (diameter of pier elements)

converge to the reference result, as demonstrated in Fig. 5.11. In fact, the average estimate coincides with the reference value, which was directly obtained by Monte Carlo simulation with the same number of samples as used in the previous case.

The sample average of the failure probability elasticities in terms of the number of independent simulation runs is shown in Fig. 5.12. For comparison, the results obtained by Monte Carlo simulation are also shown in the figure (with a square symbol). It is seen that the sample average of the elasticity coefficients stabilizes very fast to the reference result. Thus, the estimate obtained by the proposed sensitivity measure is practically unbiased. The corresponding sample coefficient of variation of the estimates, based on 20 independent runs, is given in parentheses in Tables 5.5 and 5.6. The trend of the probability of failure and the sensitivity measure in terms of the threshold is shown in Figs. 5.13 and 5.14, respectively. The results corresponding to the mean value of the diameter of the pile elements are shown in Fig. 5.13, while Fig. 5.14 shows the results related to the mean value of the diameter of the pier elements. An average of 20 independent runs is considered in the figures, where the threshold level is normalized by the acceptable relative displacement response level

Table 5.5 Sensitivity measures in terms of partial derivatives. $(\cdot\%)$ sample coefficient of variation. Failure event F_2

Average value (c.o.v.)
$\frac{\partial P_{F_2}}{\partial \mu_{D_p}}$ -2.73×10^{-2} (33%)
$\frac{\partial P_{F_2}}{\partial \mu_{D_c}}$ -3.30×10^{-3} (37%)

Table 5.6 Sensitivity measures in terms of elasticity coefficients. $(\cdot\%)$ sample coefficient of variation. Failure event F_2

Average value (c.o.v.)
$e^{F_2}_{\mu_{D_p}}$ -11.79 (18%)
$e^{F_2}_{\mu_{D_c}}$ -18.64 (14%)

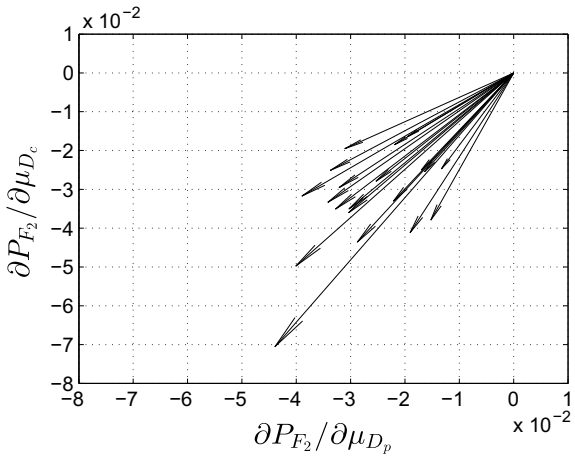

Fig. 5.10 Sensitivity of the failure probability P_{F_2} with respect to the mean value of the diameter of the pier and pile elements: 20 independent estimations

equal to 0.07 m (see Sect. 5.8.3). Once again, it is clear from the figures that the elasticity coefficients increase in magnitude as the threshold increases and, therefore, the failure probability becomes more sensitive as the failure probability becomes smaller.

5.8.7 Results: Failure Event F_3

The results of the reliability sensitivity analysis associated with the failure event related to the maximum relative displacement between the deck girder and the base of the rubber bearings at each abutment are given in Tables 5.7 and 5.8.

Table 5.7 shows the sensitivity analysis in terms of the partial derivatives of the failure probability with respect to the mean value of the system parameters D_r and H_r, while Table 5.8 gives the corresponding sensitivity measures in terms of the

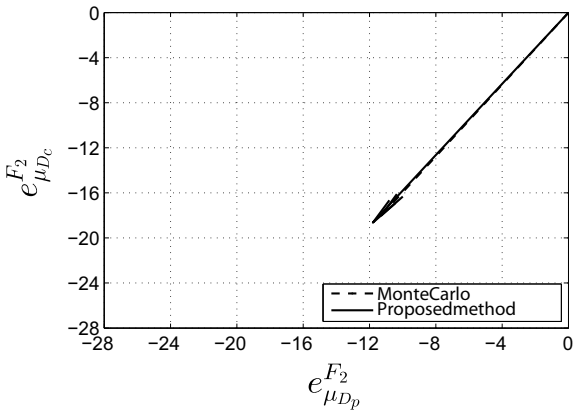

Fig. 5.11 Average of the elasticity coefficient estimates generated by the proposed approach from 20 simulation runs compared to the reference estimate (Monte Carlo). Failure event F_2. System parameters D_p and D_c

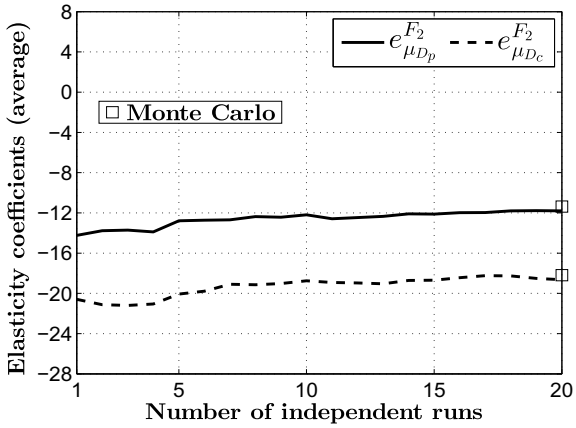

Fig. 5.12 Sample average of elasticity coefficients corresponding to the probability of failure event F_2 in terms of the number of independent simulation runs

elasticity coefficients. The information is also shown in Fig. 5.15 in form of arrows indicating the magnitude and sign of the sensitivity. As in the previous cases, the results are based on 20 independent runs.

From the tables, it is seen that the sensitivity of the failure probability with respect to the mean value of the external diameter D_r is negative. Thus, an increase in the external diameter of the isolators decreases the probability of failure. This is reasonable since the base isolation system becomes stiffer and, therefore, the relative displacement between the deck girder and the base of the rubber bearings tends to decrease. On the other hand, the sensitivity of the failure probability with respect to the mean value of the total height of rubber H_r is positive. In this case, an increase in the total height of rubber in the isolator increases the probability of failure. This is consistent with the fact that the isolation system becomes more flexible increasing in this manner the relative displacement between the deck girder and the rubber bearings. The corresponding elasticity coefficients indicate that the external diameter of the isolators plays a significant role in affecting the probability of failure. These

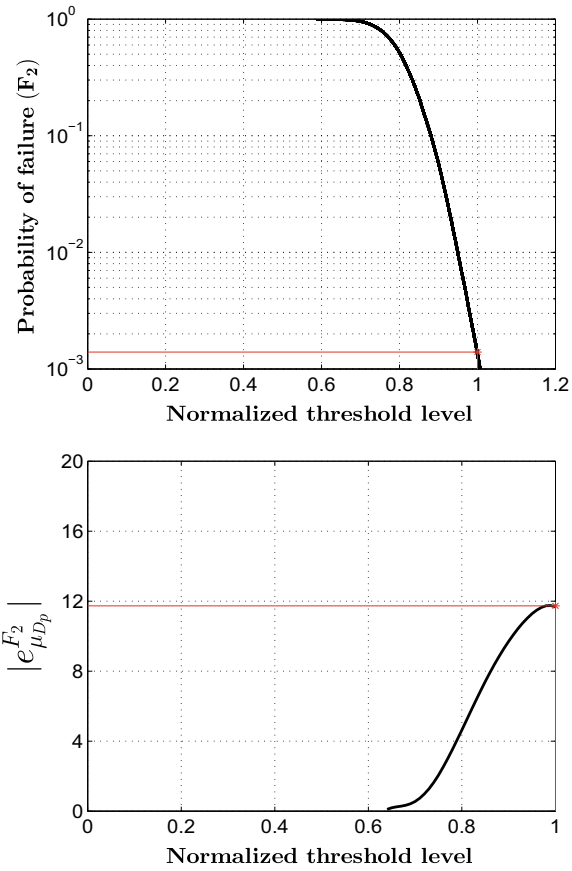

Fig. 5.13 Upper figure: Probability of failure event F_2 in terms of the normalized threshold. Lower figure: Elasticity coefficient of failure probability P_{F_2} in terms of the normalized threshold. Average of five independent runs. System parameter D_p

observations give a valuable insight into the interaction and effect of the isolator parameters on the failure event associated with the maximum relative displacement between the deck girder and the base of the rubber bearings.

As in the previous cases, the average estimates obtained by the proposed approach coincide with the reference values as shown in Fig. 5.16. Information about the sample behavior of the failure probability elasticities in terms of the number of independent simulation runs is shown in Fig. 5.17. This figure shows the sample average of the elasticity with respect to the mean value of the system parameters D_r and H_r.

It is seen that the average stabilizes extremely fast. For comparison, the results obtained by Monte Carlo simulation are also shown in the figure (with a square symbol). The average of the elasticity coefficients coincides with the Monte Carlo results. This result indicates that the sensitivity estimation in terms of the elasticity coefficients is practically unbiased, as in the previous cases. The corresponding sample coefficient of variation is shown in Fig. 5.18. The coefficient of variation of the elasticity of the failure probability with respect to the external diameter D_r and the total height of rubber H_r tends to 5% and 17%, respectively (number in parentheses

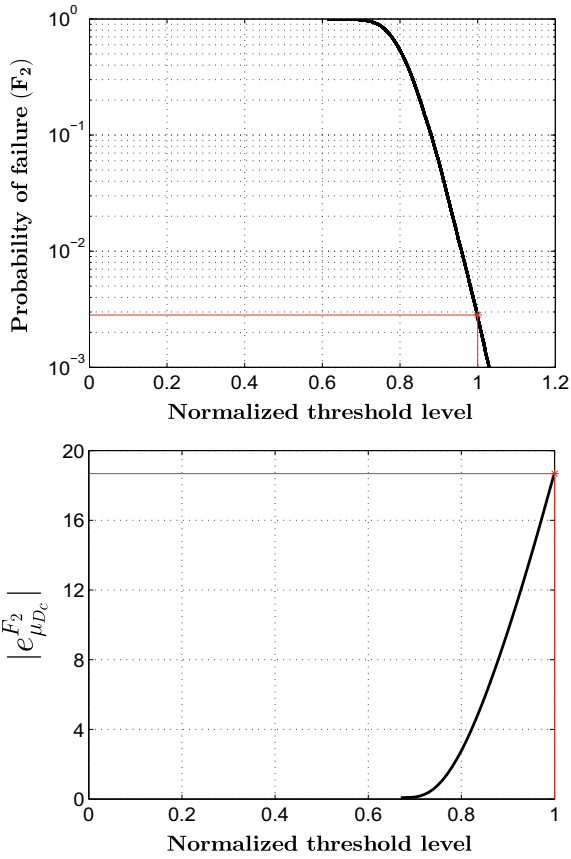

Fig. 5.14 Upper figure: Probability corresponding to failure event F_2 in terms of the normalized threshold. Lower figure: Elasticity coefficient of failure probability P_{F_2} in terms of the normalized threshold. Average of five independent runs. System parameter D_c

Table 5.7 Sensitivity measures in terms of partial derivatives. $(\cdot\%)$ sample coefficient of variation. Failure event F_3

Average value (c.o.v.)
$\frac{\partial P_{F_3}}{\partial \mu_{D_r}}$ -9.48×10^{-1} (16%)
$\frac{\partial P_{F_3}}{\partial \mu_{H_r}}$ 3.67×10^{-1} (29%)

Table 5.8 Sensitivity measures in terms of elasticity coefficients. $(\cdot\%)$ sample coefficient of variation. Failure event F_3

Average value (c.o.v.)
$e^{F_3}_{\mu_{D_r}}$ -16.75 (5%)
$e^{F_3}_{\mu_{H_r}}$ 9.06 (17%)

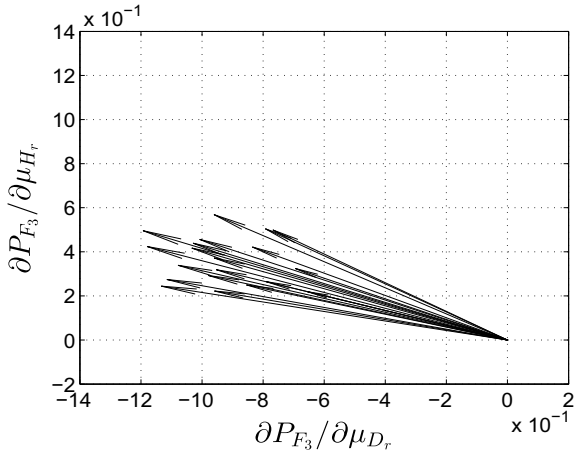

Fig. 5.15 Sensitivity of the failure probability P_{F_3} with respect to the mean value of the external diameter of the rubber bearings and the total height of rubber in the bearings: 20 independent estimations

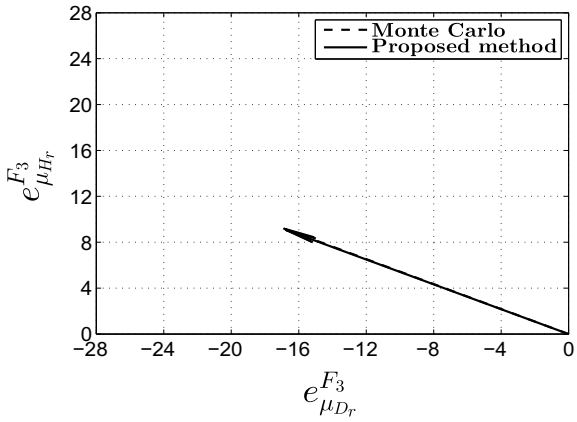

Fig. 5.16 Average of the estimates generated by the proposed approach from 20 simulation runs compared to the reference estimate (Monte Carlo). Failure event F_3. System parameters D_r and H_r

in Table 5.8). These small values correspond to the actual variability of the failure probability elasticity estimates.

The trend of the probability of failure and the sensitivity measure in terms of the threshold is shown in Figs. 5.19 and 5.20, respectively. The results corresponding to the mean value of the external diameter of the rubber bearings are shown in Fig. 5.19, while Fig. 5.20 shows the results related to the mean value of the total height of rubber in the bearings. An average of 20 independent runs is considered in the figures, where the threshold is normalized by the acceptable relative displacement response level equal to 0.10 m (see Sect. 5.8.3).

As in the previous failure events, the elasticity coefficients increase in magnitude as the threshold level increases and, therefore, the failure probability becomes more sensitive as the failure probability becomes smaller. The importance of the external diameter of the rubber bearings on failure event F_3, compared to the total height of rubber, can also be seen from the probability curves of the previous figures. In

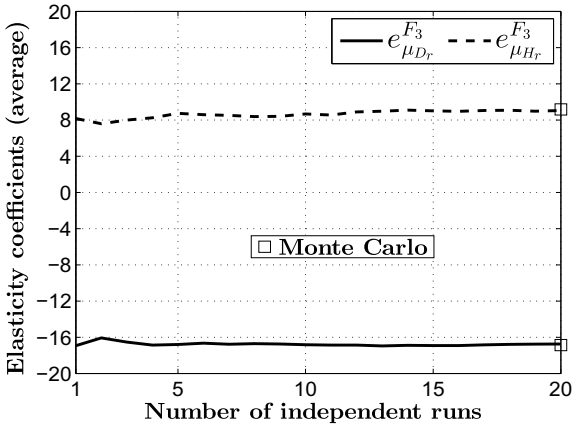

Fig. 5.17 Sample average of elasticity coefficients corresponding to the probability of failure event F_3 in terms of the number of independent simulation runs

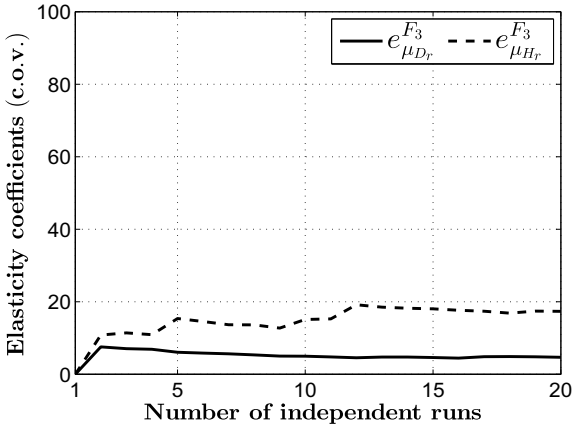

Fig. 5.18 Sample coefficient of variation of elasticity coefficients corresponding to the probability of failure event F_3 in terms of the number of independent simulation runs

fact, the probability of failure considering the external diameter of the bearings as uncertain is estimated as $P_{F_3} = 4.5 \times 10^{-2}$, for a normalized threshold equal to one, while a probability of failure $P_{F_3} = 6.5 \times 10^{-3}$ is obtained when the total height of rubber in the bearings is considered as uncertain. Note that the difference is almost one order of magnitude.

In summary, the previous results corresponding to the different failure events represent valuable and practical information about the global performance of the bridge model.

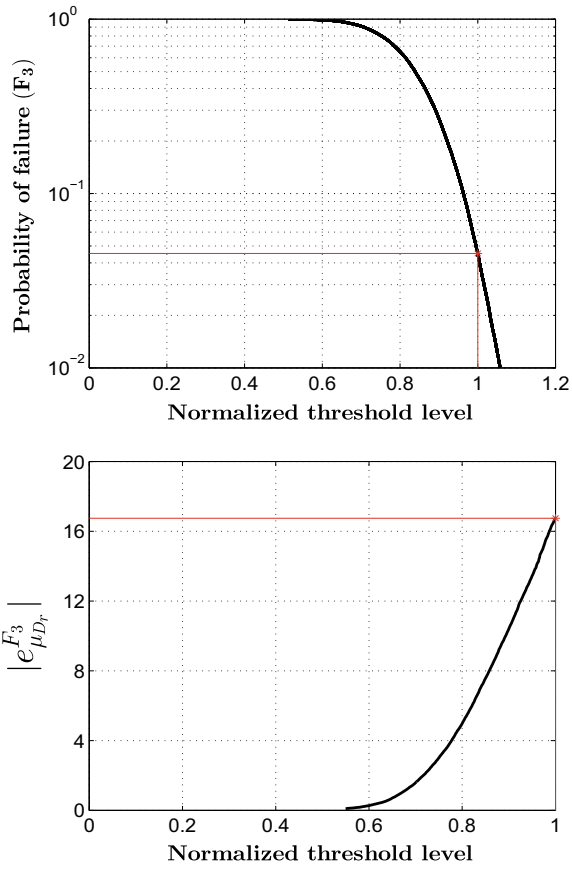

Fig. 5.19 Upper figure: Probability of failure event F_3 in terms of the normalized threshold. Lower figure: Elasticity coefficient of failure probability P_{F_3} in terms of the normalized threshold. Average of five independent runs. System parameter D_r

5.8.8 Computational Cost

The number of finite element runs required during the reliability sensitivity analysis mainly depends on the number of simulations needed by the proposed approach. Such a number is related to the number of levels or stages carried out by subset simulation. Thus, the computational effort for assembling the finite element model and obtaining its nonlinear dynamic response for a given set of system parameters is the fundamental factor for comparison purposes. In this regard, the proposed model reduction technique is quite effective. In fact, the execution time for assembling the reduced-order model represents 0.03% of the time required for the original unreduced finite element model. Overall, the use of the reduced-order model for estimating the reliability sensitivity measures results in a drastic reduction of the computational effort of almost two orders of magnitude. In other words, the ratio of the execution time for obtaining the reliability sensitivity measures by using the full finite element model and the execution time for obtaining the reliability sensitivity measures by using the reduced-order model is about 90 in this case. Thus, a significant reduction in

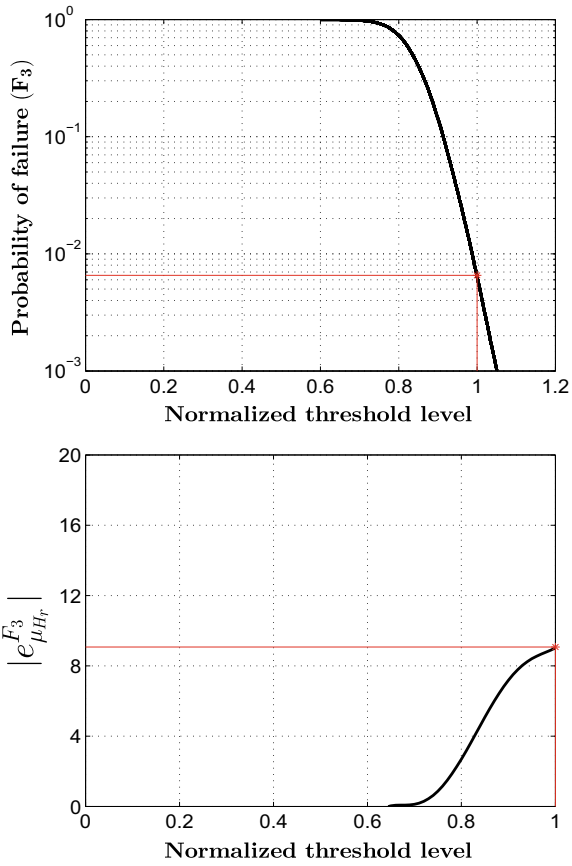

Fig. 5.20 Upper figure: Probability of failure event F_3 in terms of the normalized threshold. Lower figure: Elasticity coefficient of failure probability P_{F_3} in terms of the normalized threshold. Average of five independent runs. System parameter H_r

computational effort is achieved without compromising the accuracy of the reliability sensitivity estimates.

References

1. S.K. Au, Reliability-based design sensitivity by efficient simulation. Comput. Struct. **83**(14), 1048–1061 (2005)
2. H.-G. Beyer, B. Sendhoff, Robust optimization - a comprehensive survey. Comput. Methods Appl. Mech. Eng. **196**(33–34), 3190–3218 (2007)
3. P. Bjerager, S. Krenk, Parametric sensitivity in first order reliability theory. J. Eng. Mech. **115**(7), 1577–1582 (1989)
4. J. Ching, Y.H. Hsieh, Local estimation of failure probability function and its confidence interval with maximum entropy principle. Probab. Eng. Mech. **22**(1), 39–49 (2007)
5. O. Ditlevsen, H.O. Madsen, *Structural Reliability Methods* (Wiley, Chichester, 1996)
6. I. Doltsinis, Z. Kang, Robust design of structures using optimization methods. Comput. Methods Appl. Mech. Eng. **193**(23–26), 2221–2237 (2004)

7. V. Dubourg, B. Sudret, Meta-model-based importance sampling for reliability sensitivity analysis. Struct. Saf. **49** (2014)
8. H.A. Jensen, Design and sensitivity analysis of dynamical systems subjected to stochastic loading. Comput. Struct. **83**, 1062–1075 (2005)
9. H.A. Jensen, D. Kusanovic, M. Papadrakakis, Reliability-based characterization of base-isolated structural systems, in *European Congress on Computational Methods in Applied Sciences and Engineering. ECCOMAS 2012*, Vienna, Austria, 10–14 September 2012
10. H.A. Jensen, D.S. Kusanovic, On the effect of near-field excitations on the reliability-based performance and design of base-isolated structures. Probab. Eng. Mech. **36**, 28–44 (2014)
11. H.A. Jensen, F. Mayorga, M.A. Valdebenito, Reliability sensitivity estimation of nonlinear structural systems under stochastic excitation: a simulation-based approach. Comput. Methods Appl. Mech. Eng. **289**, 1–23 (2015)
12. H.A. Jensen, F. Mayorga, C. Papadimitriou, Reliability sensitivity analysis of stochastic finite element models. Comput. Methods Appl. Mech. Eng. **296**, 327–351 (2015)
13. A. Karamchandani, C.A. Cornell, Sensitivity estimation within first and second order reliability methods. Struct. Saf. **11**(2), 95–107 (1992)
14. J.M. Kelly, Aseismic base isolation: review and bibliography. Soil Dyn. Earthq. Eng. **5**(4), 202–216 (1986)
15. N.H. Kim, H. Wang, N.V. Queipo, Adaptive reduction of design variables using global sensitivity in reliability-based optimization. Int. J. Reliab. Saf. **1**(1–2), 102–119 (2006)
16. P.S. Koutsourelakis, Design of complex systems in the presence of large uncertainties: a statistical approach. Comput. Methods Appl. Mech. Eng. **197**(49–50), 4092–4103 (2008)
17. D.A. Kusanovic, Reliability-Based Characterization of Base-Isolated Buildings. MSc thesis, National Technical University of Athens, Institute of Structural Analysis and Seismic Research, School of Civil Engineering, Greece, 2013
18. B.M. Kwak, T.W. Lee, Sensitivity analysis for reliability-based optimization using an AFOSM method. Comput. Struct. **27**(3), 399–406 (1987)
19. M. Lemaire, A. Chateauneuf, J.-C. Mitteau, *Structural Reliability* (Wiley, New York, 2009)
20. Z. Lu, S. Song, Z. Yue, J. Wang, Reliability sensitivity method by line sampling. Struct. Saf. **30**(6), 517–532 (2008)
21. N. Makris, S. Chang, Effects of Damping Mechanisms on the Response of Seismically Isolated Structures. PEER report 1998/06. Berkeley (CA): Pacific Earthquake Engineering Research Center. College of Engineering, University of California, 1998
22. R.E. Melchers, M. Ahammed, A fast approximate method for parameter sensitivity estimation in Monte Carlo structural reliability. Comput. Struct. **82**(1), 55–61 (2004)
23. S. Minewaki, M. Yamamoto, M. Higashino, H. Hamaguchi, H. Kyuke, T. Sone, H. Yoneda, Performance tests of full size isolators for super high-rise isolated buildings. J. Struct. Eng. AIJ **55**(B), 469–477 (2009)
24. S. Rahman, D. Wei, Design sensitivity and reliability-based structural optimization by univariate decomposition. Struct. Multidiscip. Optim. **35**(3), 245–261 (2008)
25. R.Y. Rubinstein, D.P. Kroese, *Simulation and Monte Carlo Method* (Wiley, New York, 2007)
26. G.I. Schuëller, H.A. Jensen, Computational methods in optimization considering uncertainties – an overview. Comput. Methods Appl. Mech. Eng. **198**(1), 2–13 (2008)
27. S. Song, Z. Lu, H. Qiao, Subset simulation for structural reliability sensitivity analysis. Reliab. Eng. Syst. Saf. **94**(2), 658–665 (2009)
28. L. Su, G. Ahmadi, J.G. Tadjbakhsh, A comparative study of performances of various base isolation systems, part II: sensitivity analysis. Earthq. Eng. Struct. Dyn. **19**, 21–33 (1990)
29. A.A. Taflanidis, G. Jia, A simulation-based framework for risk assessment and probabilistic sensitivity analysis of base-isolated structures. Earthq. Eng. Struct. Dyn. **40**(14), 1629–1651 (2011)
30. M.A. Valdebenito, H.A. Jensen, G.I. Schuëller, F.E. Caro, Reliability sensitivity estimation of linear systems under stochastic excitation. Comput. Struct. **92–93**, 257–268 (2012)
31. Y.T. Wu, Computational methods for efficient structural reliability and reliability sensitivity analysis. AIAA J. **32**(8), 1717–1723 (1994)

32. M. Yamamoto, S. Minewaki, M. Higashino, H. Hamaguchi, H. Kyuke, T. Sone, H. Yoneda, Performance tests of full size rubber bearings for isolated superhigh-rise buildings, in *International Symposiumon Seismic Response Controlled Buildings for Sustainable Society*, Tokyo, Japan, 2009
33. M. Yamamoto, S. Minewaki, H. Yoneda, M. Higashino, Nonlinear behavior of high-damping rubber bearings under horizontal bidirectional loading: full-scale test and analitycal modeling. Earthq. Eng. Struct. Dyn. **41**(13), 1845–1860 (2012)
34. E. Zio, N. Pedroni, Monte Carlo simulation-based sensitivity analysis of the model of a thermal-hydraulic passive system. Reliab. Eng. Syst. Saf. **107**, 90–106 (2012)